NUREG/CR-2767
SAND82-1292
R3
Printed November 1982

X-Ray Measurements of Water Fog Density

Allen L. Camp

Prepared by
Sandia National Laboratories
Albuquerque, New Mexico 87185 and Livermore, California 94550
for the United States Department of Energy
under Contract DE-AC04-76DP00789

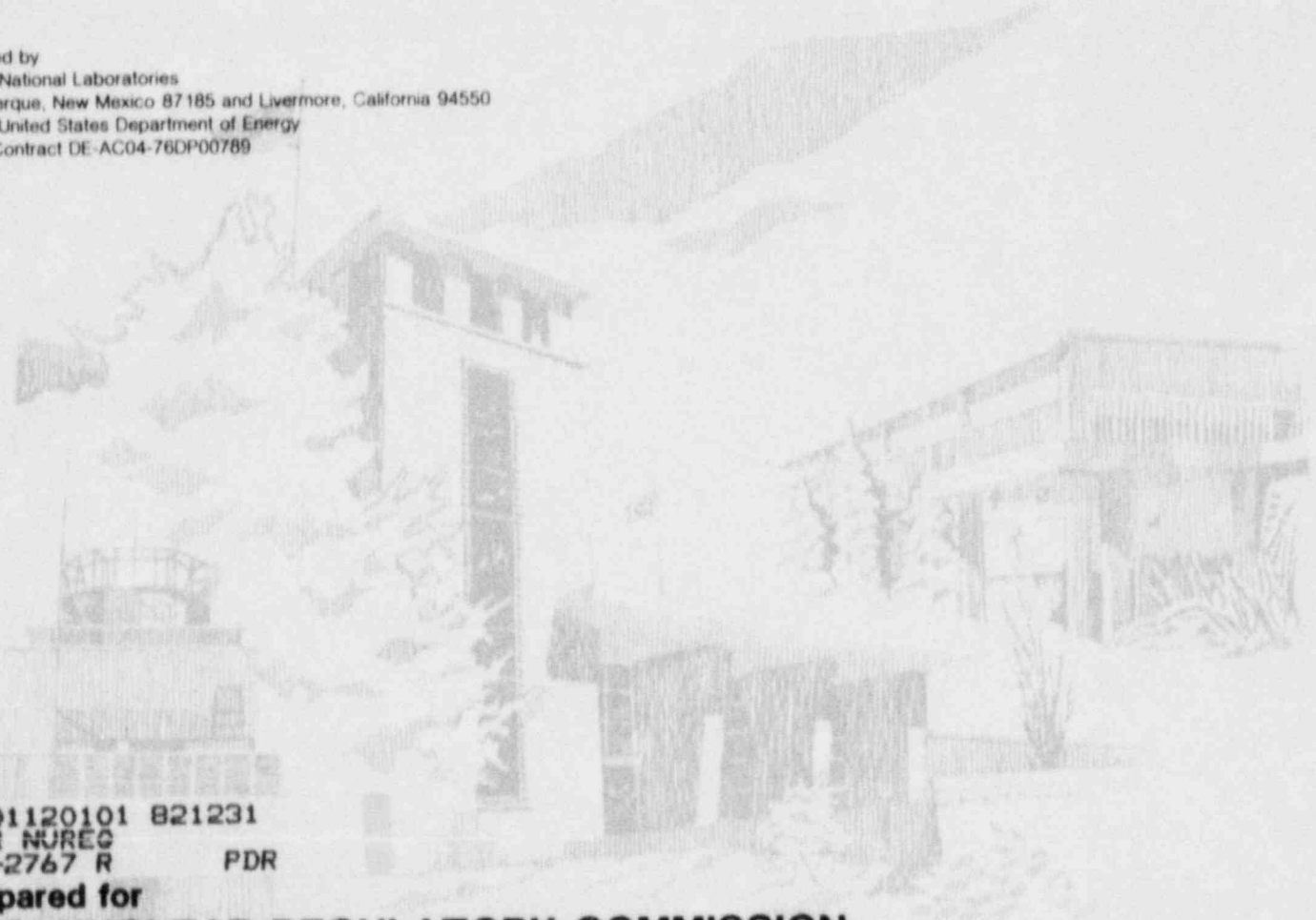

Prepared for
U. S. NUCLEAR REGULATORY COMMISSION

Available from

GPO Sales Program
Division of Technical Information and Document Control
U.S. Nuclear Regulatory Commission
Washington, D.C. 20555

and

National Technical Information Service
Springfield, Virginia 22161

NUREG/CR-2767
SAND82-1292
R3

X-RAY MEASUREMENTS OF WATER FOG DENSITY

Allen L. Camp

Sandia National Laboratories
Albuquerque, NM 87185
Operated by
Sandia National Laboratories
for the
U. S. Department of Energy

October 1982

Prepared for
Division of Accident Evaluation
Office of Nuclear Regulatory Research
U. S. Nuclear Regulatory Commission
Washington, DC 20555
Under Memorandum of Understanding DOE 40-550-75
NRC FIN No. A-1246

ABSTRACT

Water fog densities were measured in a laboratory experiment using x-ray diagnostics. Fog densities were measured, varying the flow rate, nozzle type, nozzle configuration, nozzle height above the x-ray beam, and water surface tension. Suspended water volume fractions between 0.0006 and 0.0074 percent were measured. The fog density increases approximately as the square root of the flow rate; the other parameters had little effect on the density.

TABLE OF CONTENTS

ACKNOWLEDGMENTS

The author would like to thank the following people whose assistance was instrumental in the success of this effort:

J. E. Shepherd and O. B. Crump, who designed and set up the experimental apparatus;

K. M. Gilbert, D. W. Tipping, and J. E. Silva, who provided and operated the x-ray machine; and

M. Berman and M. P. Sherman, who provided advice and assistance during the experiment.

SUMMARY

Previous analytical work indicates that water fogs may significantly reduce the pressures encountered during a hydrogen burn. For a fog to be effective, water volume fractions above 0.01 percent and drop radii below about 200 μm are recommended.

We have performed a series of laboratory experiments to measure the density of water fogs with a low energy, high intensity x-ray beam. The fog density was measured, varying the flow rate, nozzle type, nozzle configuration, nozzle height above the x-ray beam, and surface tension. Suspended water volume fractions between 0.0008 and 0.0074 percent were measured.

We found the water fog density to be primarily a function of flow rate. The density varied as the square root of the flow rate, indicating significant agglomeration. Decreasing the mass mean drop radius from 200 μm to 50 μm appears to increase the density by a factor of 2 or 3. Further reductions to 25 μm had little or no effect. Factors such as height and surface tension had little effect. Extrapolation of the experimental data to full-scale applications indicates that flow rates higher than those normally encountered in nuclear reactor containments would be required to achieve the desired fog density.

I. INTRODUCTION

Since the accident at Three Mile Island, concern has been raised that some nuclear reactors may not be adequately prepared to deal with hydrogen combustion during severe accidents. Because of this concern, the Nuclear Regulatory Commission asked Sandia National Laboratories to investigate hydrogen behavior and control in light water reactors. This effort includes evaluating various mitigation schemes for reactors that appear particularly susceptible to problems of hydrogen combustion.

Some mitigation schemes previously proposed include inerting (pre- or post-accident), deliberate ignition, and deliberate ignition coupled with water fogs or foams. Deliberate ignition coupled with water fogs or foams is particularly attractive because the hydrogen is removed during combustion and much of the energy released is dissipated by evaporating water, greatly reducing the rise in temperature and pressure of the containment atmosphere.

Calculations indicate that water fogs with densities above about 0.01 volume percent and with drops below about 200 μm in radius will produce significant temperature and pressure reductions.[1] The major concern with water fogs is that losses due to droplet agglomeration may make a sufficiently high fog density unattainable with "reasonable" flow rates.

As a first step in ascertaining the feasibility of water fogs, we have conducted a set of laboratory-scale water fog density measurements. Many techniques for examining water fogs exist, including photographic methods, laser techniques, hot-wire anemometry, and x-ray methods. This particular set of experiments used x-ray diagnostics, due to the simplicity of the method and the availability of the equipment. While x-rays are very useful for determining the density of the fog, no drop-size information can be obtained. Drop-size information will be gathered in future experiments with lasers and other equipment. The x-ray experiments, in addition to providing insight into the question of fog maintenance, will provide benchmark data for future experiments.

Chapter II presents a background discussion of the potential benefits of water fogs and the expected problems. Chapter III discusses the theory behind the x-ray measurements. Chapter IV describes the test plan and experimental apparatus. Chapter V presents the experimental results, and Chapter VI presents the conclusions and recommendations.

II. BACKGROUND

A combination of water fogs and deliberate ignition has been proposed as a mitigation scheme for hydrogen combustion.[1] The hydrogen would be burned to remove it from containment, and the energy released by combustion would be dissipated by evaporating water drops, greatly reducing the rise in temperature and pressure of the containment atmosphere. Figures 1 and 2 show the theoretical pressures and temperatures expected for the complete, adiabatic, constant-volume combustion of hydrogen:air mixtures with various water fog densities.[1] Examination of Figure 1 indicates that water fog densities in excess of 0.01 volume percent will produce significant pressure reductions. For example, Figure 1 shows that a final pressure to initial pressure ratio of 3 can be obtained with the combustion of less than 5 volume percent hydrogen, if no drops are present. If a 0.05 volume percent water fog is present, it takes 16 volume percent hydrogen to produce the same pressure ratio of 3.

In order for a water fog to be effective, the drops must evaporate on a time scale that is shorter than or comparable to the total burn time. Figure 3 shows the vaporization time versus droplet radius for various combustion conditions.[1] If we conservatively assume that the drops should evaporate in one second or less, it appears that drops with radii below about 200 μm would be adequate.

While the advantages of a water fog are obvious, there is some question as to whether or not it is feasible to produce and maintain a high density fog in a containment. The major concern with water fogs is that losses due to droplet agglomeration may make a sufficiently high fog density unattainable with "reasonable" flow rates. Agglomeration losses occur when drops collide and coalesce. The collisions normally occur when larger drops, with higher terminal velocities, overtake smaller drops, with lower terminal velocities. If the colliding drops coalesce, the resultant larger drop will fall at a velocity higher than either of the original drops. Thus, the rate of water loss increases. A more detailed discussion of this subject can be found in Reference 1.

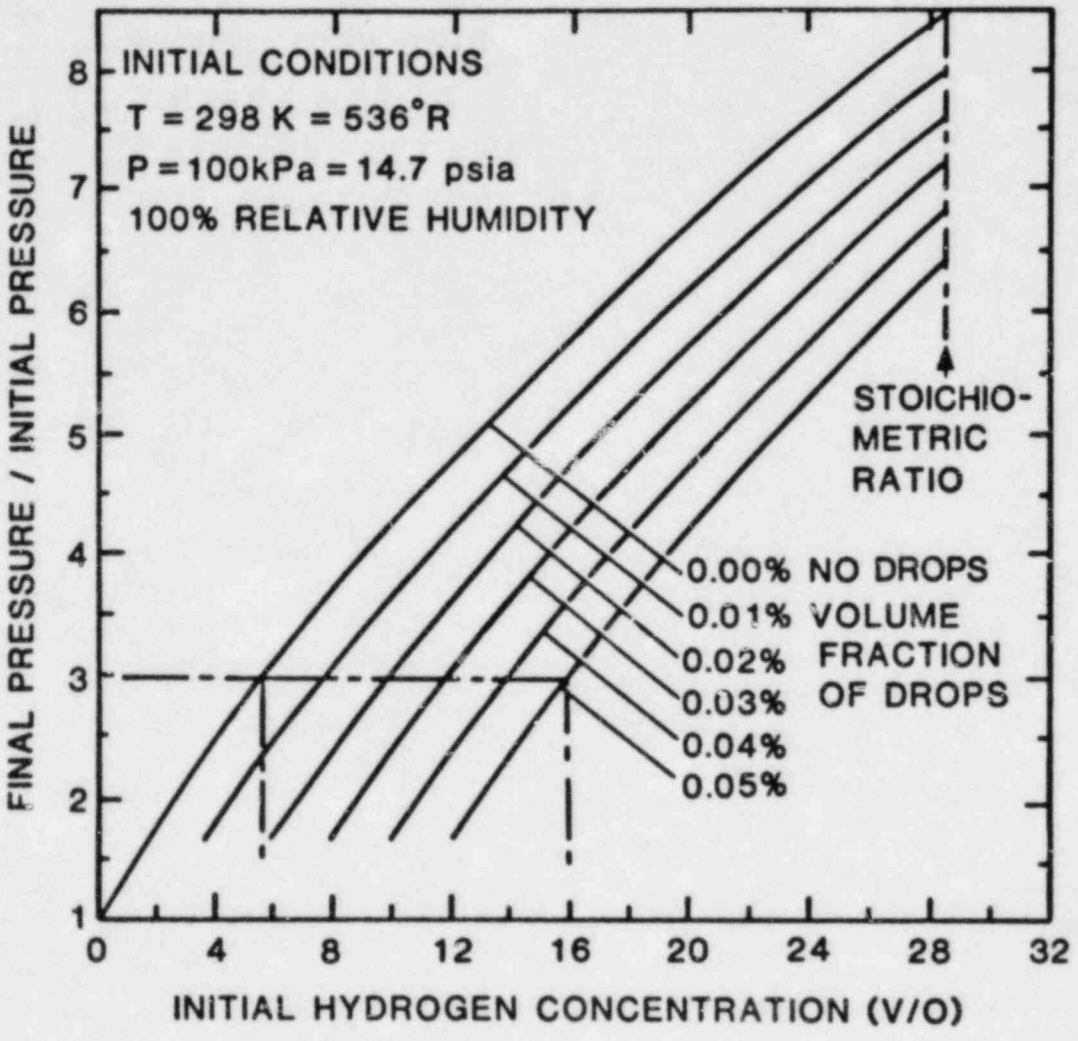

Figure 1. Ratio of final pressure to initial pressure as a function of initial hydrogen concentration and volume fraction of water drops

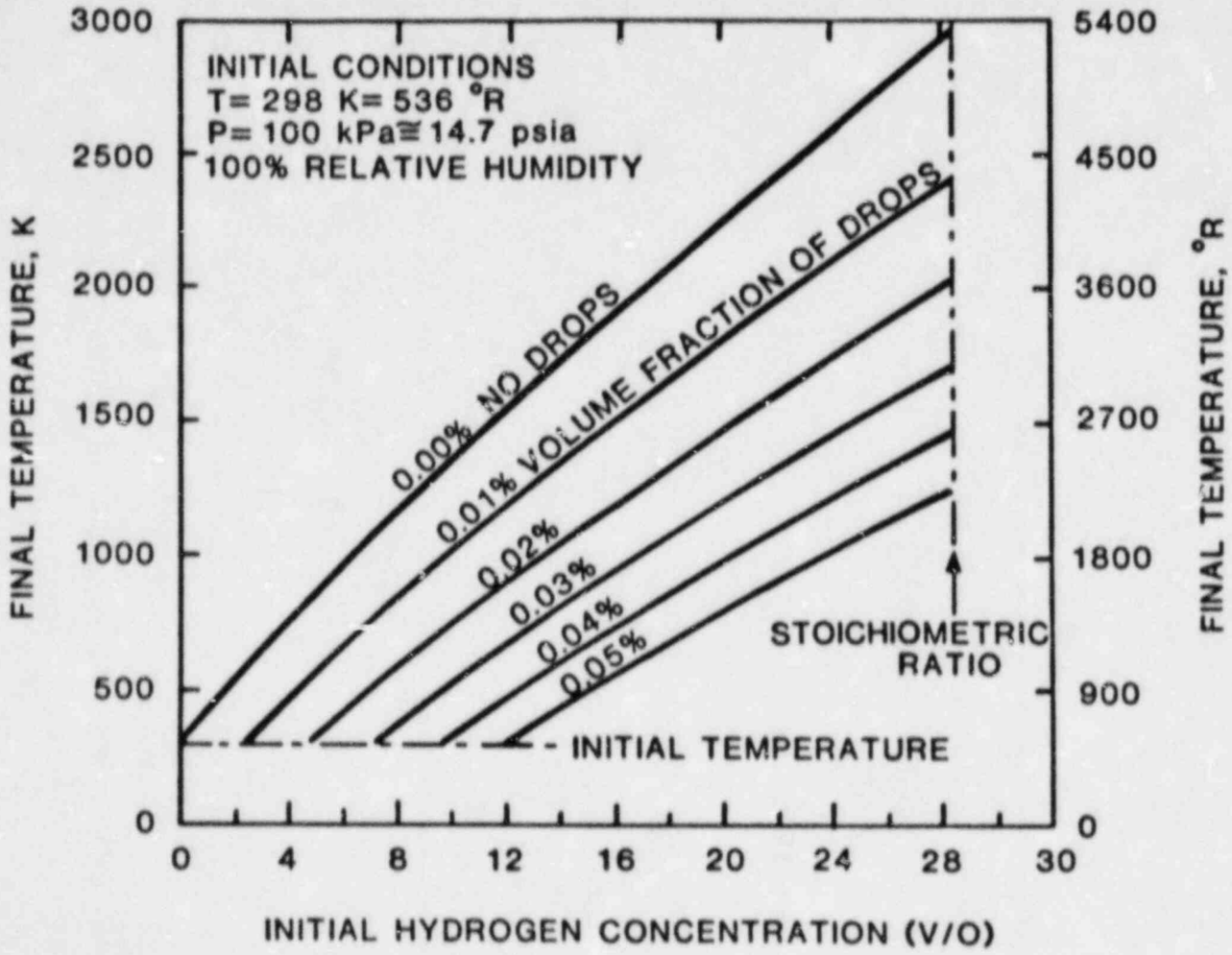

Figure 2. Final temperature as a function of initial hydrogen concentration and volume fraction of water drops

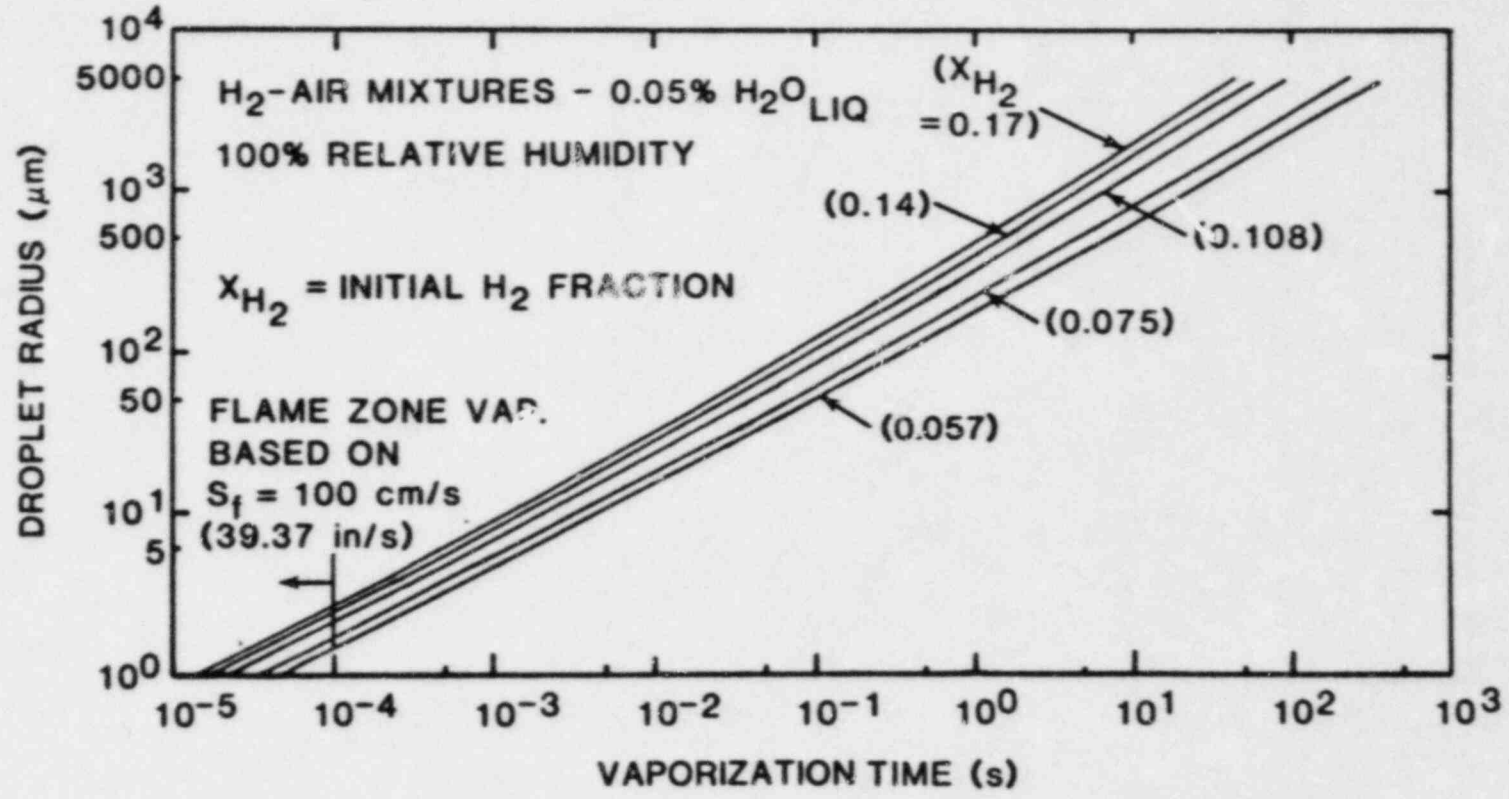

Figure 3. Vaporization Time vs. Droplet Radius at Various Combustion Stoichiometries

III. THEORY

In our experiments, the water fog density was measured with a high intensity 6.4 KeV x-ray beam. At this low x-ray energy, Compton scattering of the x-rays is negligible, and the photoelectric effect dominates the attenuation. The 6.4 KeV x-ray beam was generated with a Henke x-ray system using an iron fluorescer.[2] In order to simplify the density calculations, we made the following assumptions:

1. displacement of air by the water fog was negligible
2. the air density and humidity were constant during each measurement.

The fog density can then be determined from the following expression:

$$\rho = \ell n(T)/\mu X \qquad (1)$$

where

ρ = fog density, kg/m^3 ($10^3 kg/m^3 \approx 100$ volume percent)

T = transmissivity = $\frac{\text{count rate with fog}}{\text{count rate without fog}}$

(Count rates are corrected for background)

μ = absorption coefficient for water = 1.9893 m^2/kg

X = beam length = 1.302 m

Equation (1) also assumes that no self shielding is occurring. This can be a problem in experiments involving discrete particles, such as water drops. Self shielding occurs because the back of the particle is shielded somewhat from the x-ray flux and, therefore, does not contribute as much as it should to the attenuation. The attenuation correlation presented in equation (1) is derived for a slab of constant thickness, and any deviation from that geometry will lead to decreased attenuation due to self shielding. However, because most of the drops in this experiment are estimated to have a radius less than 100 μm, and the mean free path of 6.4 KeV x-rays in water is about 500 μm, self shielding is negligible.

Assuming steady-state conditions and no air motion, the density is a function of the mass flow rate and the velocity as shown in equation (2)

$$\rho(h) = \int_0^\infty \frac{\dot{m}(r,h)dr}{Av(r,h)} \qquad (2)$$

where

$\rho(h)$ = fog density at a distance h from the nozzles

$m(r,h)$ = mass flow rate of drops of radius r at a distance h from the nozzles

A = cross sectional area of flow

$v(r,h)$ = velocity of drops of radius r at a distance h from the nozzle.

For our measurements to be meaningful, h should be large enough that most of the drops have slowed down to their terminal velocity. Otherwise, densities will be measured that are too low.

The droplet velocity can be calculated from:

$$\frac{dv}{dt} = \frac{g(\rho_L - \rho_g)}{\rho_L} \quad \frac{\pi r^2 v^2 \rho_g C_D}{2m} \qquad (3)$$

where

v = velocity

t = time

g = gravitation constant

ρ_L = liquid density

ρ_g = air density

r = droplet radius

C_D = drag coefficient (function of velocity)

m = mass

The velocity at the nozzle is assumed to be

$$v_o = \frac{\dot{m}}{\rho_L A} \qquad (4)$$

where

$\dot{m}$ = mass flow rate

A = area of nozzle orifice

A discussion of calculations performed with equations (3) and (4) is presented with the results.

IV. TEST PLAN AND DESCRIPTION OF APPARATUS

The experiments were designed to examine the effects of changing the following parameters:

- nozzle type
- nozzle configuration
- nozzle height above the beam
- flow rate

Additionally, we investigated the effect of adding a surfactant to the water to reduce surface tension.

The experimental setup is shown in Figures 4-12. The aluminum stall has floor dimensions 1.52 m x 1.52 m and is 1.83 m high. Note in Figure 7 that the design of the x-ray and detector ports includes air flow to prevent the fog from drifting into the ports and getting on the equipment. This particular design alleviated any concern about water films that could bias the attenuation calculations. The size of the aluminum stall was limited by the space in the room, but was large enough to provide a beam length through the fog of 1.30 m and a maximum fall height from the nozzles to the beam of 1.28 m. Figures 10 and 11 show the nozzle arrangements for the 1, 6 and 12 nozzle configurations. The nozzles used were the Spraco hollow-cone nozzle #16080804, the Spraco full-cone nozzle #11062004, the Spraco hollow-cone nozzle #1713A (see Figure 12). These nozzles are assumed to produce drops with a log-normal distribution and mass mean radii of approximately 25, 50, and 200 μm, respectively.*

Any changes in the air density in the stall during a measurement will cause an error in the experiment. Changes in temperature, pressure, and relative humidity can cause significant errors. The relative humidity was maintained near 100 percent by operating the sprays for a period of time before the background measurements were taken. No attempt was made to control room temperature or pressure; however, the temperature in the stall was recorded for most tests. Any concern that drops from one experiment would remain suspended in the air long enough to bias the results of the next experiment was alleviated by waiting a minimum of three minutes between experiments.

*Based upon estimates supplied by Spraco.

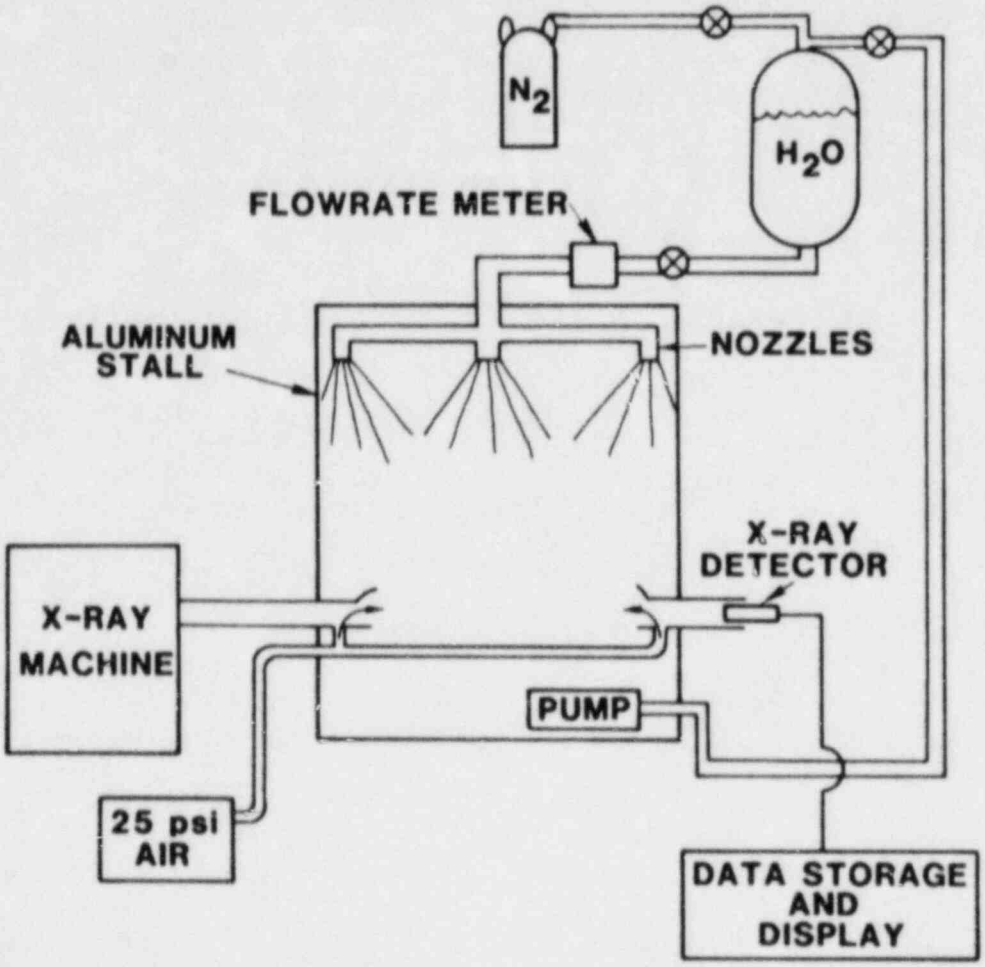

Figure 4. X-ray Experiment Schematic

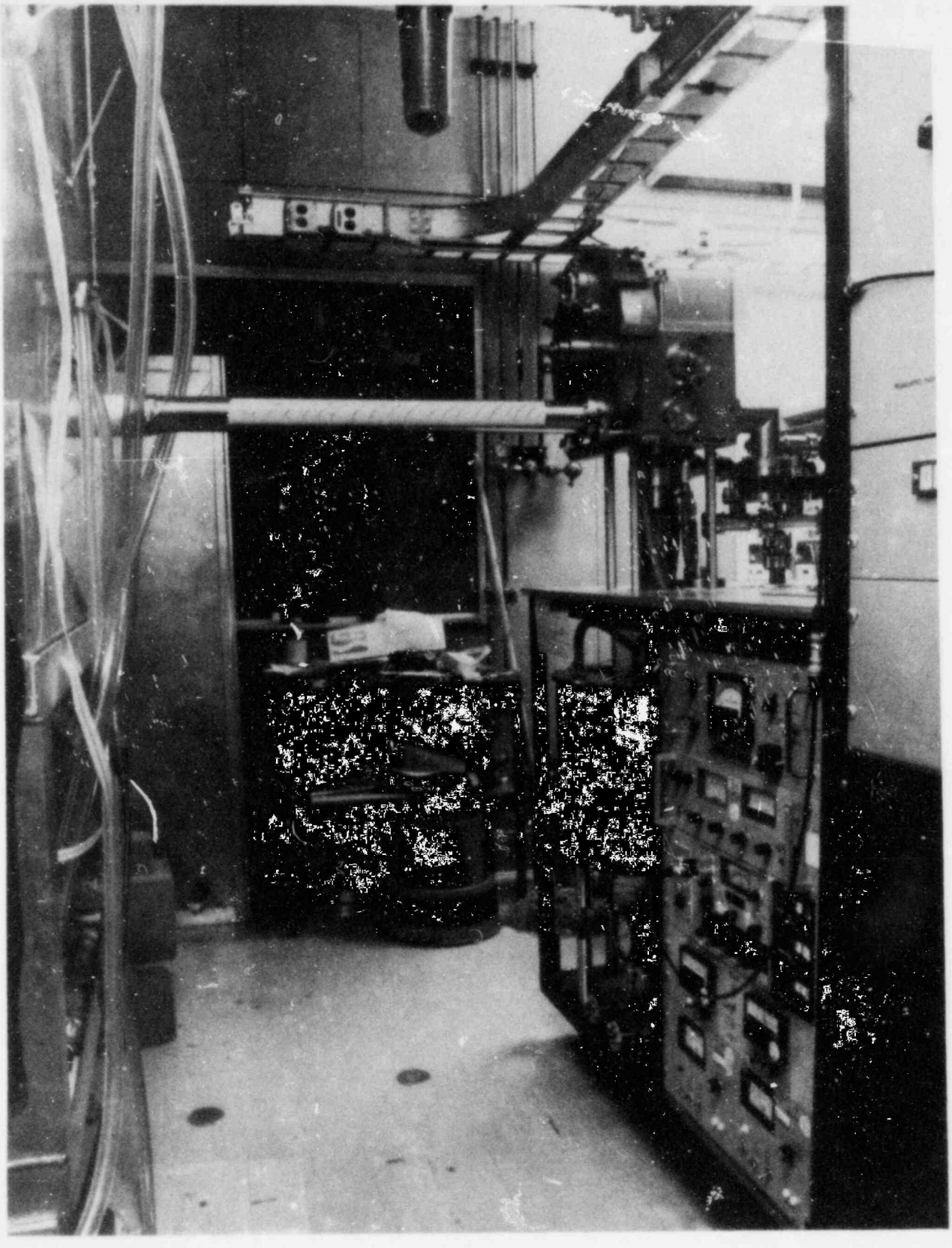

Figure 5. Henke x-ray Machine and Beam Tube

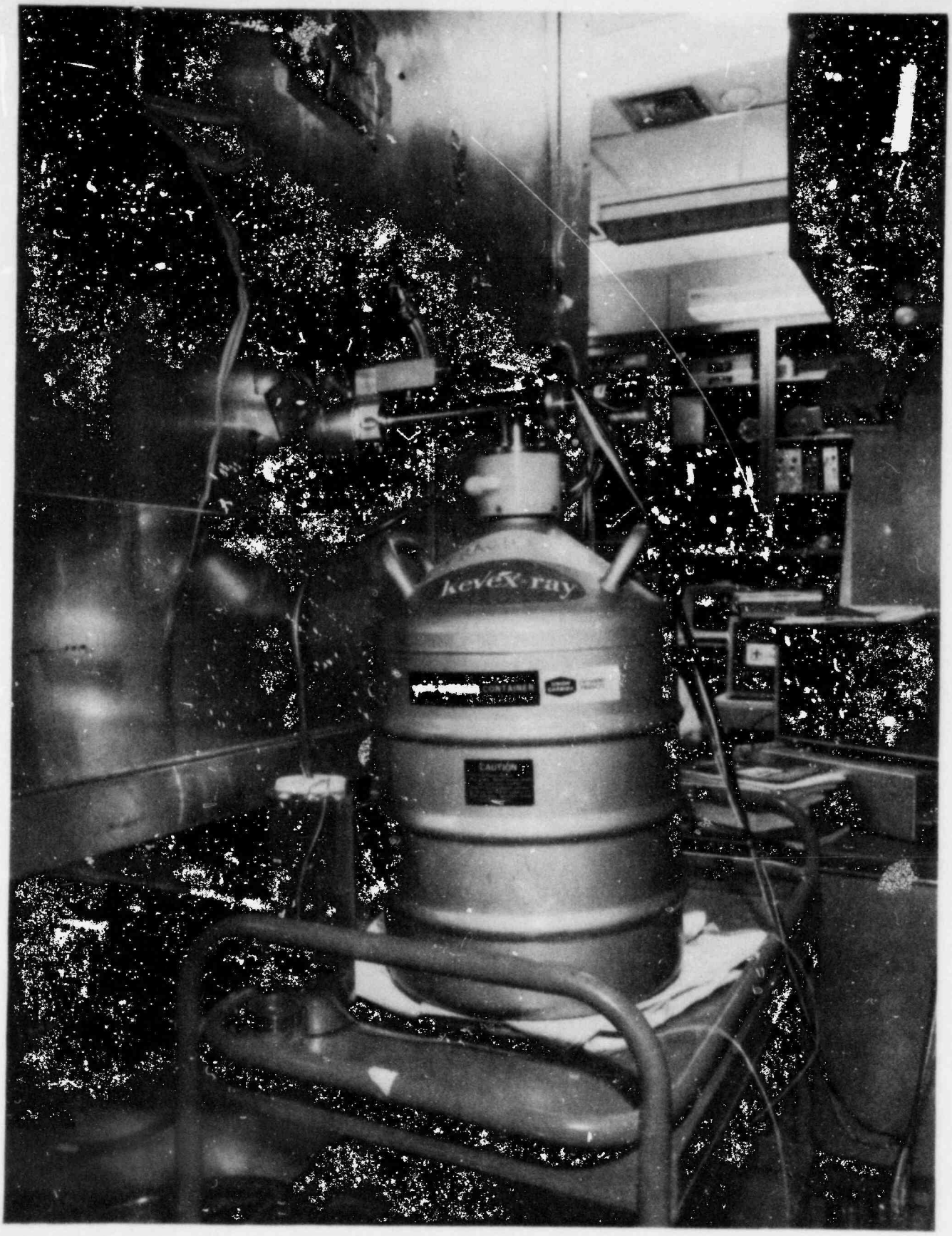

Figure 6. SiLi Detector Arrangement

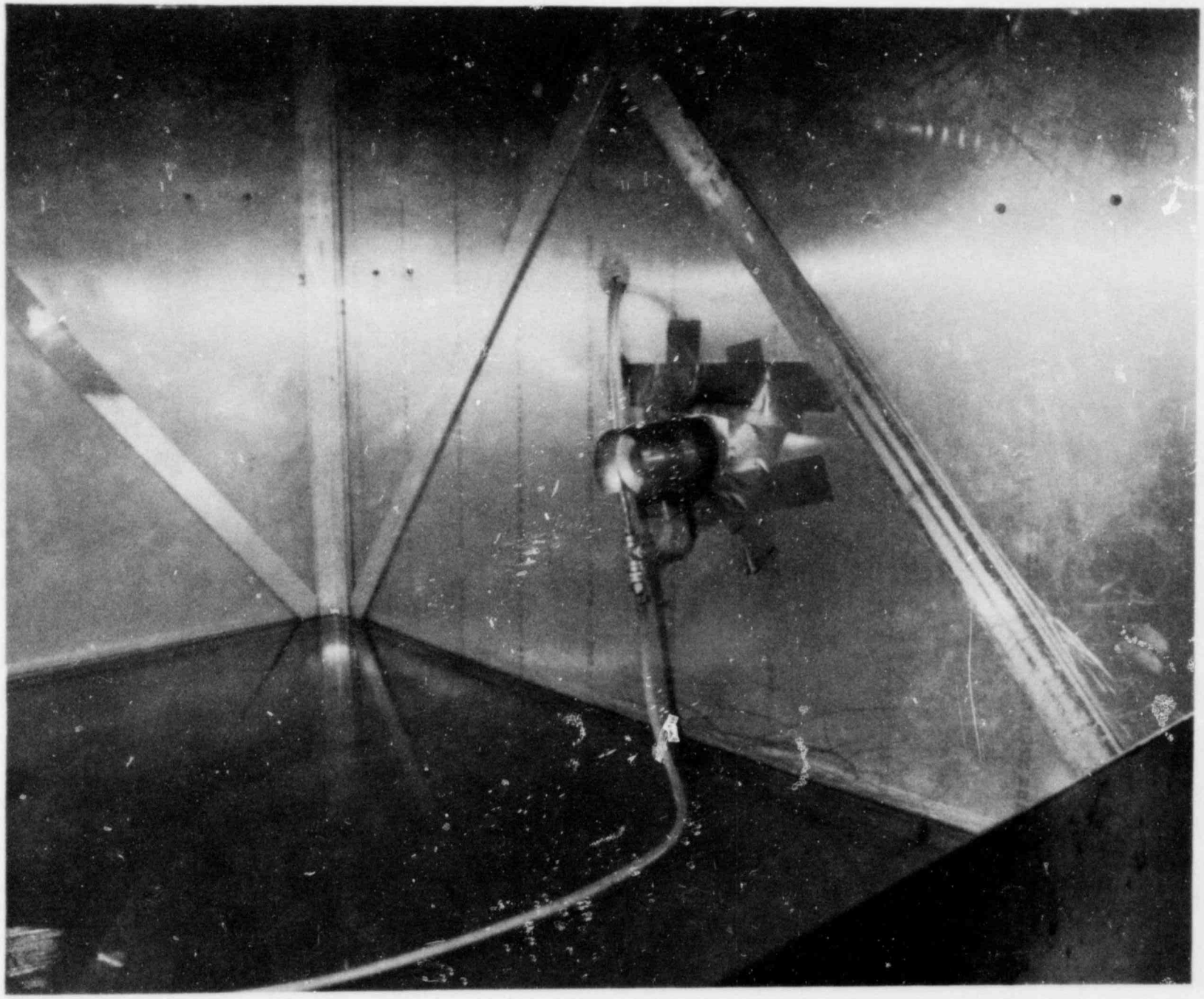

Figure 7. Beam Port Including Air Supply

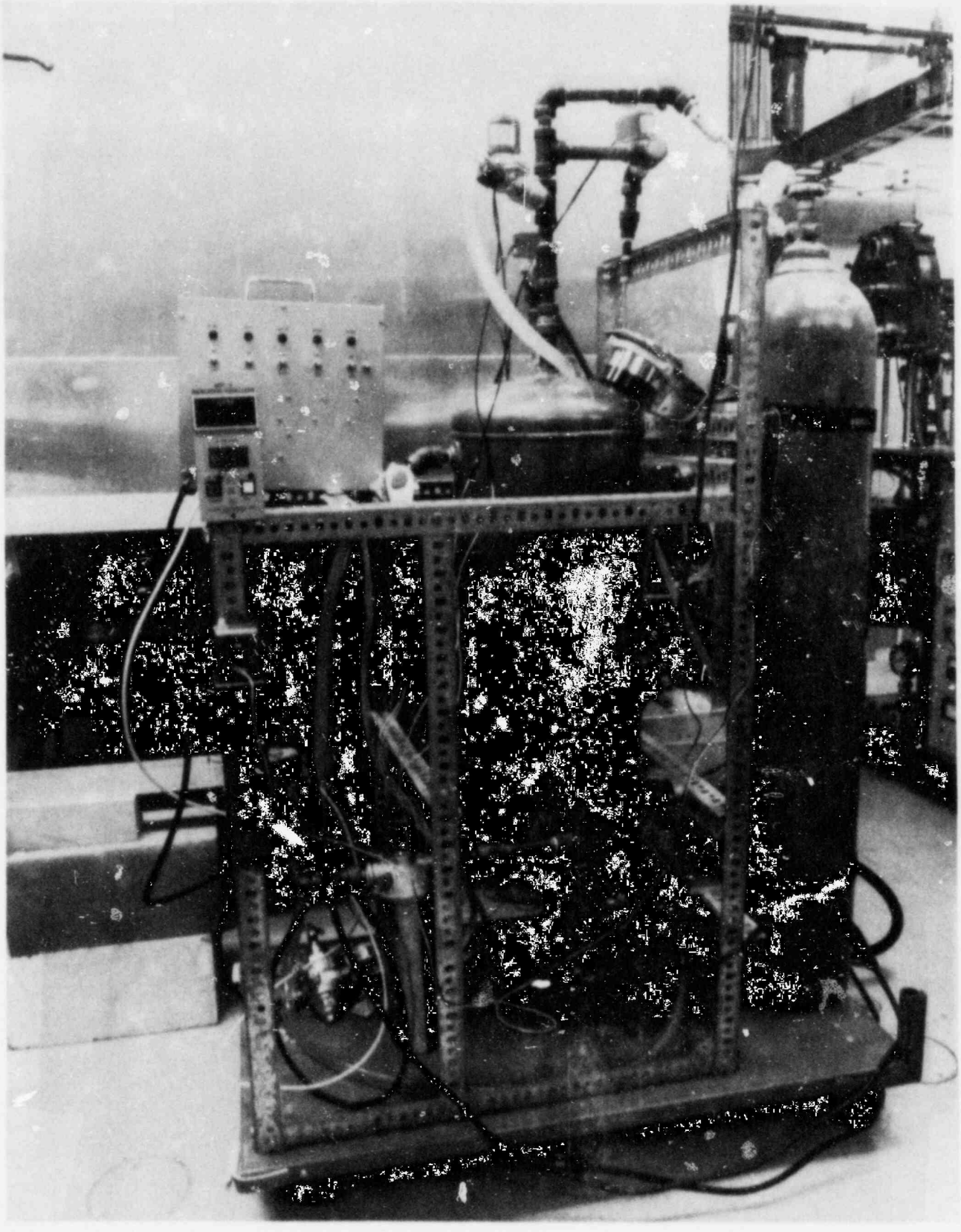

Figure 8. Water Supply Including Storage Tank, N_2 Bottle, and Flowmeter

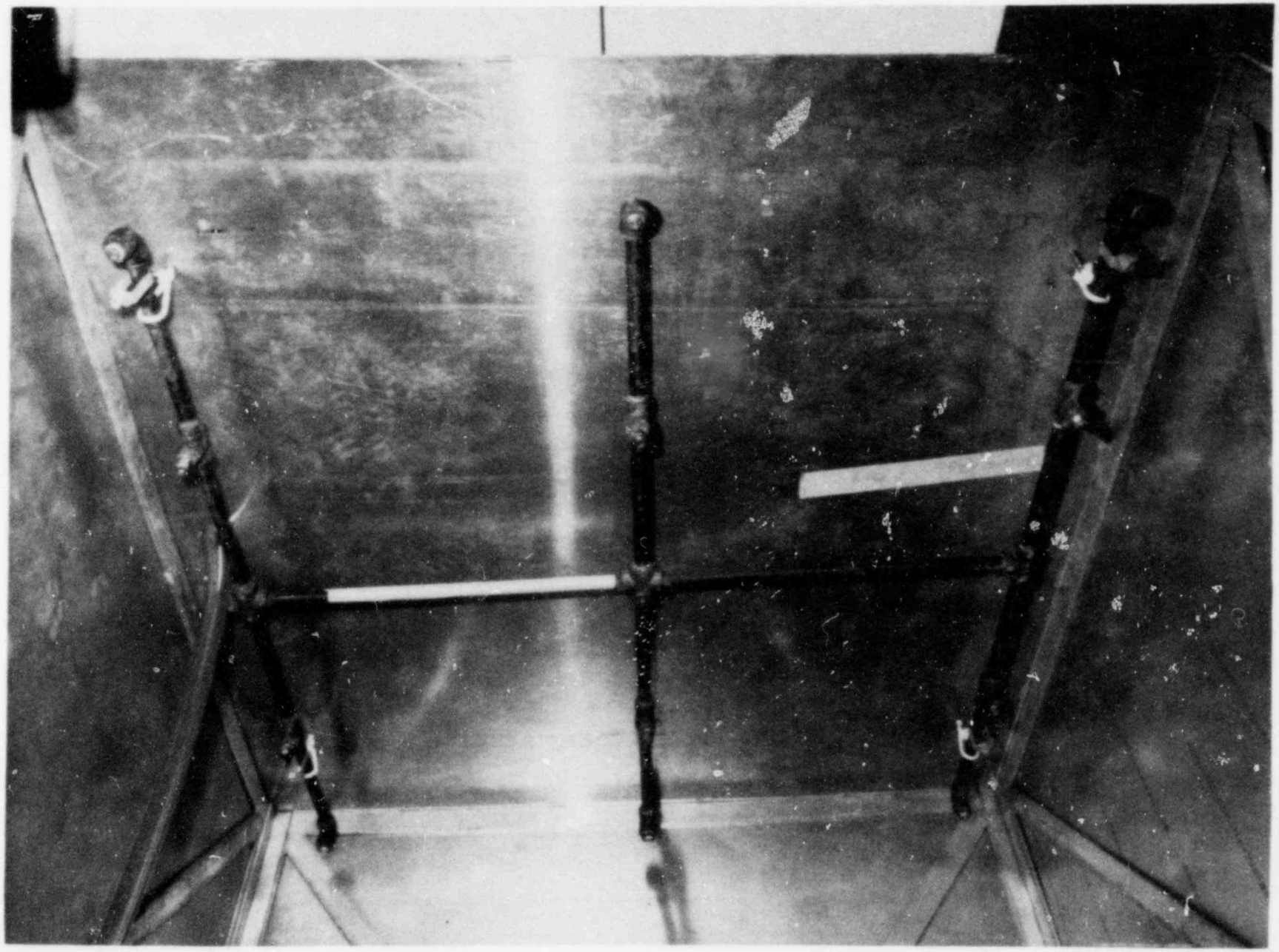

Figure 9. Nozzle Maniford Arrangement

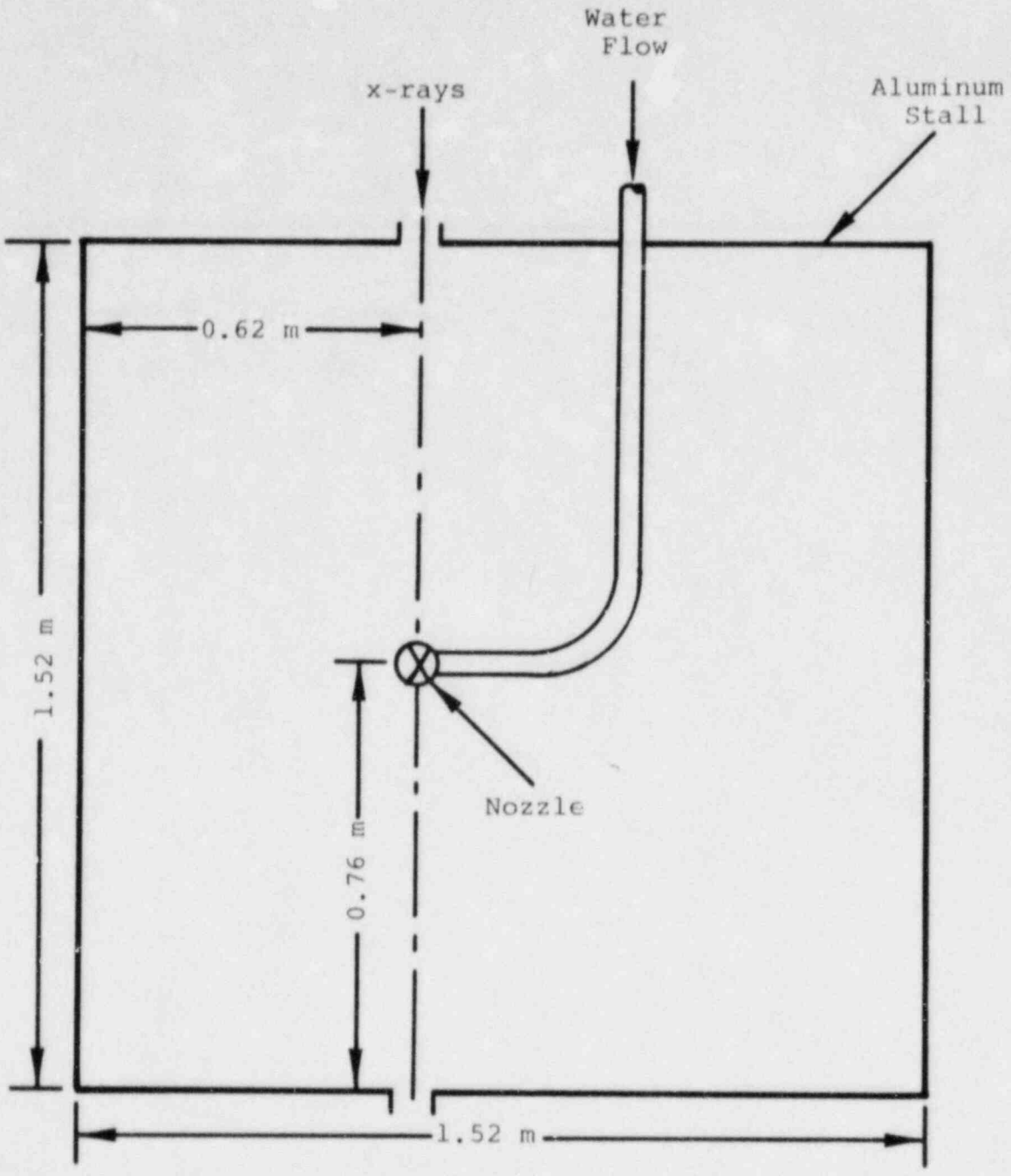

Figure 10. Schematic of the Single Nozzle Configuration

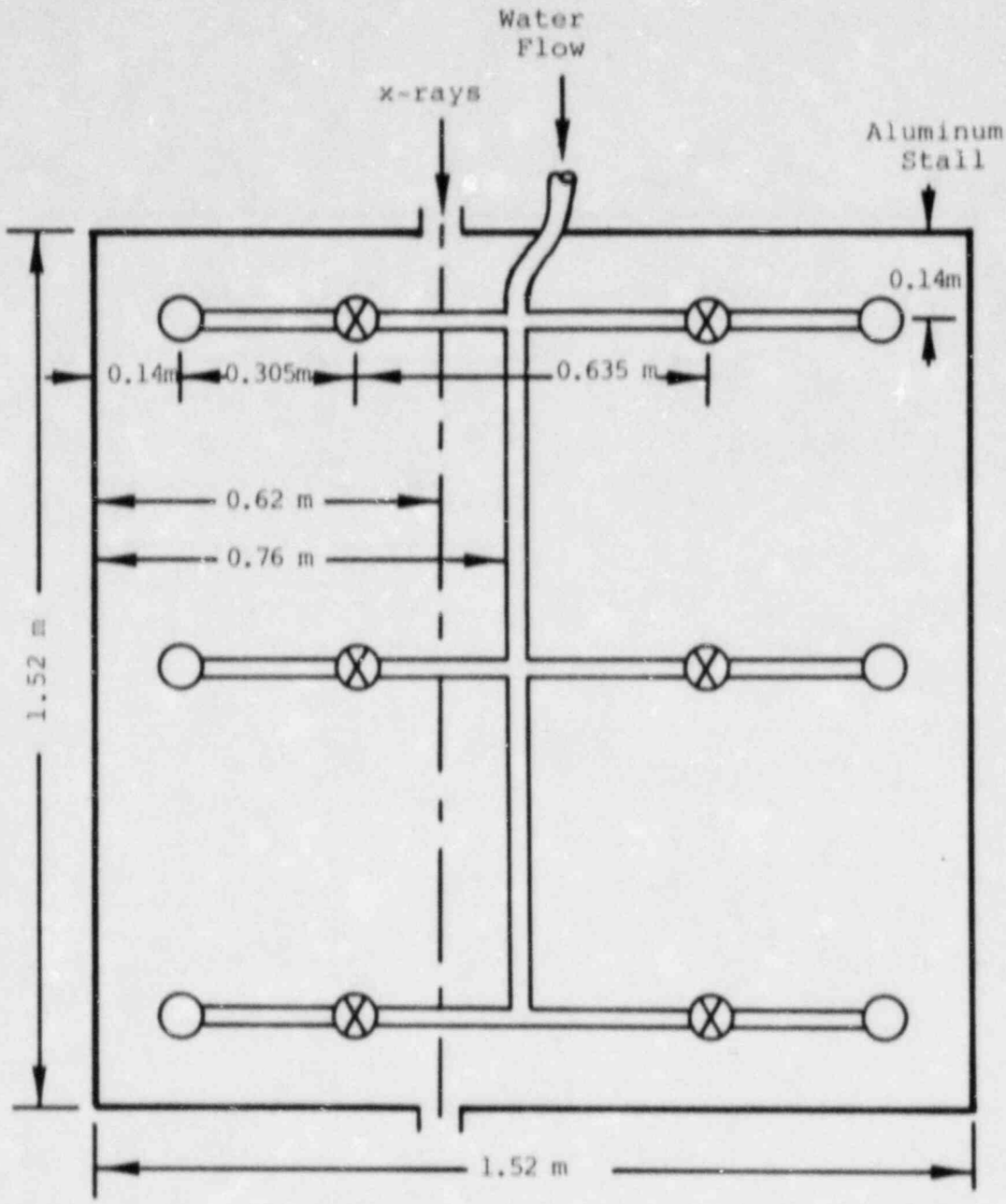

Figure 11. Six and Twelve Nozzle Configurations.

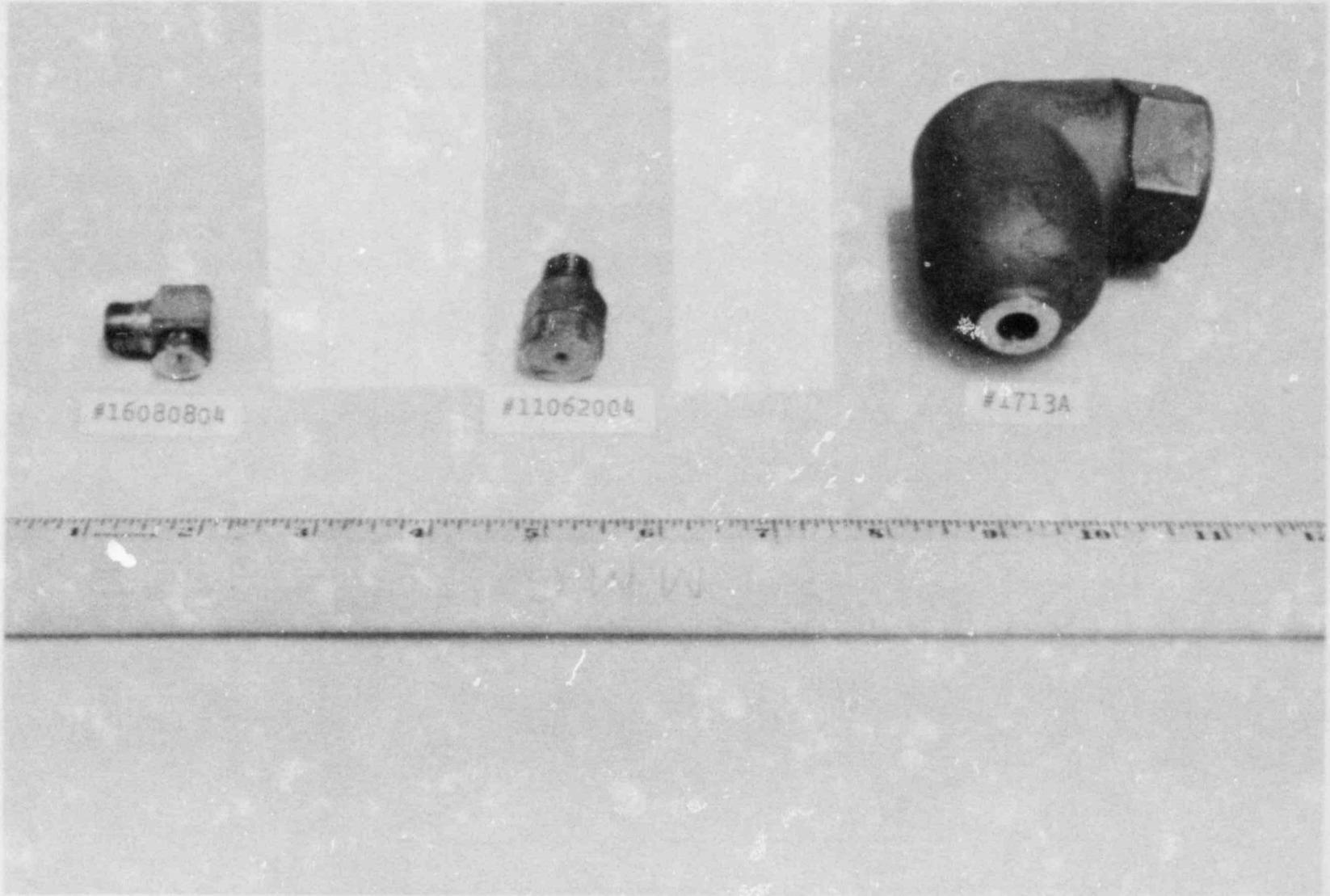

Figure 12. Nozzles

V. RESULTS

The results are shown in Tables 1-8. Measurement error in the tables has been reported in three ways. For each data point, errors due to counting statistics are presented. However, some fluctuations in the data outside of statistical uncertainty are observed. These are the result of changes in air density, fluctuations in flow rate, x-ray machine drift, etc. The mean density for each experimental configuration is accompanied by the standard deviation and the measured total spread in the data.

Results for Nozzles #16080804 and #11062004

Tables 1-3 show the results for the Spraco hollow-cone nozzle #16080804. The mass-mean drop radius for these nozzles is estimated to be 25 μm. Tables 4-6 show the results for the Spraco full-cone nozzles #11062004. The mass-mean drop radius for these nozzles is estimated to be 50 μm. Tables 1-6 and Figure 13 show that the fog density is primarily a function of flow rate for these two types of nozzles. The density appears to vary as the square root of the flow rate (as predicted in Reference 1). This indicates that significant agglomeration has occurred, otherwise the density would vary linearly with flow rate.[1] For these nozzles and at this small scale, changes in droplet fall distance and a factor of two difference in mean drop size appear to have little effect. The small decreases in density that are observed with increasing droplet fall distance may be due to either increasing wall losses or increasing agglomeration or both.

Calculations using equations (3) and (4) indicate that the drops reach terminal velocity soon after leaving the nozzles and well before the drops reach the x-ray beam. Visual observations indicate that the fog is reasonably well mixed about 60 cm below the nozzles.

One anomaly does appear in the data. The data for fall distances of 1.00 and 1.26 m (Table 6) do not reflect the expected increase in density when the flow rate is increased. The cause of this anomaly is not known at this time.

If we assume that extrapolation of the data in Figure 13 is valid, then we can estimate the flow rates required to maintain a high density fog in a containment building. The following equation represents the curve in Figure 13.

TABLE 1

Data for Single Nozzle #16080804 Centered Above X-Ray Beam

Test #	Height Above Beam m	Driving Pressure MPa	Flow Rate x 10^6 m^3/s	Temperature ^oC	Density* x 10^2 kg/m^3	Standard Deviation x 10^2	Total Spread x 10^2
161	.77	1.034	5.68	23	1.22 ± 6.1%		
162	.77	1.034	5.68	23	.955 ± 7.8%		
163	.77	1.034	5.68	23	1.15 ± 6.5%		
Mean	.77	1.034	5.68	23	1.11	.14	.27
164	.77	1.276	6.94	23	1.10 ± 6.8%		
165	.77	1.276	6.94	23	1.10 ± 6.6%		
Mean	.77	1.276	6.94	23	1.12	.02	.03
166	1.03	1.034	5.68	23	.766 ± 9.8%		
167	1.03	1.034	5.68	22	1.17 ± 6.4%		
168	1.03	1.034	5.68	22	.863 ± 8.7%		
Mean	1.03	1.034	5.68	22	.93	.21	.40
169	1.03	1.276	6.94	22	1.12 ± 6.7%		
170	1.03	1.276	6.94	22	1.05 ± 7.1%		
Mean	1.03	1.276	6.94	22	1.09	.05	.07
173	1.28	1.034	5.68	24	1.07 ± 7.0%		
174	1.28	1.034	5.68	24	1.19 ± 6.3%		
Mean	1.28	1.034	5.68	24	1.13	.08	.12
175	1.28	1.276	6.94	24	1.33 ± 5.6%		
176	1.28	1.276	6.94	24	1.13 ± 6.6%		
177	1.28	1.276	6.94	24	1.08 ± 6.9%		
Mean	1.28	1.276	6.94	24	1.18	.13	.25

*Percent error shown in this column is due to counting statistics only.

TABLE 2

Data for Six Nozzles #16080804

Test #	Height Above Beam m	Driving Pressure MPa	Flow Rate x 10^3 m^3/s	Temperature ^oC	Density* x 10^2 kg/m^3	Standard Deviation x 10^2	Total Spread x 10^2
54	.77	1.034	.046	19	2.70 ± 4.1%		
56	.77	1.034	.046	19	2.72 ± 4.1%		
Mean	.77	1.034	.046	19	2.71	0.1	0.2
57	.77	1.034	.052	19	2.86 ± 3.9%		
58	.77	1.034	.052	19	3.03 ± 2.8%		
59	.77	1.034	.052	19	3.27 ± 2.6%		
60	.77	1.034	.052	19	2.90 ± 2.9%		
Mean	.77	1.034	.052	19	3.02	.18	.41
61	1.03	1.034	.044	19	2.59 ± 3.3%		
62	1.03	1.034	.044	19	2.72 ± 3.2%		
63	1.03	1.034	.044	19	2.87 ± 3.0%		
64	1.03	1.034	.044	19	2.79 ± 3.1%		
Mean	1.03	1.034	.044	19	2.74	.15	.28
78	1.03	1.034	.048	20	2.89 ± 3.0%		
79	1.03	1.034	.049	20	2.88 ± 3.0%		
80	1.03	1.034	.049	20	3.18 ± 2.7%		
81	1.03	1.034	.048	20	3.09 ± 2.8%		
82	1.03	1.034	.049	20	3.08 ± 2.8%		
Mean	1.03	1.034	.049	20	3.03	.13	.30
68	1.28	1.034	.042	20	2.87 ± 2.8%		
69	1.28	1.034	.042	21	2.65 ± 3.0%		
70	1.28	1.034	.042	21	2.76 ± 2.9%		
Mean	1.28	1.034	.042	21	2.76	.11	.22
71	1.28	1.034	.047	21	3.13 ± 2.6%		
72	1.28	1.034	.047	21	3.11 ± 2.9%		
Mean	1.28	1.034	.047	21	3.12	.01	.02

*Percent error shown in this column is due to counting statistics only.

TABLE 3

Data for Twelve Nozzles #16080804

Test #	Height Above Beam m	Driving Pressure MPa	Flow Rate x 10^3 m^3/s	Temperature ^oC	Density* x 10^2 kg/m^3	Standard Deviation x 10^2	Total Spread x 10^2
109	.77	1.034	.090	20	4.19 ± 3.2%		
110	.77	1.034	.090	20	4.12 ± 3.3%		
111	.77	1.034	.090	20	4.24 ± 3.2%		
Mean	.77	1.034	.090	20	4.18	.06	.12
112	.77	1.276	.099	20	4.52 ± 2.8%		
113	.77	1.276	.099	20	4.25 ± 3.0%		
114	.77	1.276	.099	20	4.41 ± 2.9%		
115	.77	1.276	.099	20	4.14 ± 3.1%		
116	.77	1.276	.099	20	4.00 ± 3.2%		
117	.77	1.276	.099	20	4.36 ± 2.9%		
Mean	.77	1.276	.099	20	4.28	.19	.52
97	1.03	1.034	.090	20	3.87 ± 3.5%		
98	1.03	1.034	.090	20	3.56 ±3.8%		
99	1.03	1.034	.090	20	3.89 ± 3.5%		
Mean	1.03	1.034	.090	20	3.77	.19	.33
91	1.03	1.276	.098	20	3.80 ± 3.6%		
92	1.03	1.276	.098	20	4.17 ± 3.3%		
93	1.03	1.276	.098	20	3.87 ± 3.5%		
95	1.03	1.276	.098	20	4.17 ± 3.3%		
96	1.03	1.276	.098	20	3.92 ± 3.5%		
Mean	1.03	1.276	.098	20	3.99	.17	.37
100	1.28	1.034	.090	20	3.12 ± 4.3%		
101	1.28	1.034	.090	20	3.33 ± 4.0%		
102	1.28	1.034	.090	20	3.22 ± 4.1%		
Mean	1.28	1.034	.090	20	3.22	.11	.21
103	1.28	1.276	.098	20	3.54 ± 3.8%		
104	1.28	1.276	.098	20	3.47 ± 3.8%		
105	1.28	1.276	.098	20	3.77 ± 3.5%		
106	1.28	1.276	.098	20	3.34 ± 4.0%		
107	1.28	1.276	.098	20	3.49 ± 3.8%		
Mean	1.28	1.276	.098	20	3.52	.16	.43

*Percent error shown in this column is due to counting statistics only.

TABLE 4

Data for Single Nozzle #11062004 Centered Above X-Ray Beam

Test #	Height Above Beam m	Driving Pressure MPa	Flow Rate x 10^3 m^3/s	Temperature ^oC	Density* x 10^2 kg/m^3	Standard Deviation x 10^2	Total Spread x 10^2
157	.75	1.034	.024	21	1.55 ± 5.4%		
158	.75	1.034	.024	21	1.54 ± 5.5%		
Mean	.75	1.034	.024	21	1.55	.01	.01
159	.75	1.276	.026	21	1.72 ± 4.9%		
160	.75	1.276	.026	21	1.70 ± 5.0%		
Mean	.75	1.276	.026	21	1.71	.01	.02
152	1.00	1.034	.023	22	1.62 ± 5.2%		
153	1.00	1.034	.023	22	1.57 ± 5.4%		
Mean	1.00	1.034	.023	22	1.60	.04	.05
154	1.00	1.276	.026	22	1.70 ± 5.0%		
155	1.00	1.276	.026	22	1.54 ± 5.5%		
156	1.00	1.276	.026	22	1.66 ± 5.1%		
Mean	1.00	1.276	.026	22	1.63	.08	1.6
147	1.26	1.034	.024	22	1.38 ± 6.1%		
148	1.26	1.034	.023	22	1.40 ± 6.0%		
Mean	1.26	1.034	.024	22	1.39	.01	.02
150	1.26	1.276	.026	22	1.60 ± 5.3%		
151	1.26	1.276	.026	22	1.60 ± 5.3%		
Mean	1.26	1.276	.026	22	1.60	0	0

*Percent error shown in this column is due to counting statistics only.

TABLE 5

Data for Six Nozzles #11062004

Test #	Height Above Beam m	Driving Pressure MPa	Flow Rate x 10^3 m^3/s	Density* x 10^2 kg/m^3	Standard Deviation x 10^2	Total Spread x 10^2
45	.75	1.034	.143	4.94 ± 3.8%		
46	.75	1.034	.143	5.16 ± 2.5%		
Mean	.75	1.034	.143	5.05	.16	.22
41	.75	1.276	.161	5.10 ± 2.6%		
42	.75	1.276	.160	5.30 ± 5.0%		
43	.75	1.276	.161	5.16 ± 5.1%		
44	.75	1.276	.161	5.21 ± 2.5%		
Mean	.75	1.276	.161	5.19	.08	.20
36	1.00	1.034	.143	4.92 ± 2.9%		
37	1.00	1.034	.146	5.02 ± 3.9%		
38	1.00	1.034	.147	5.07 ± 2.6%		
Mean	1.00	1.034	.145	5.00	.08	.15
39	1.00	1.276	.160	5.33 ± 3.5%		
40	1.00	1.276	.161	5.23 ± 2.5%		
Mean	1.00	1.276	.161	5.28	.07	.10
33	1.26	1.034	.143	4.67 ± 5.0%		
34	1.26	1.034	.145	4.89 ± 2.8%		
35	1.26	1.034	.145	5.00 ± 3.8%		
Mean	1.26	1.034	.144	4.85	.17	.33
26	1.26	1.276	.160	5.30 ± 2.2%		
27	1.26	1.276	.160	5.31 ± 3.1%		
Mean	1.26	1.276	.160	5.31	.01	.01

*Percent error shown in this column is due to counting statistics only.

TABLE 6

Data for Twelve Nozzles #11062004

Test #	Height Above Beam m	Driving Pressure MPa	Flow Rate x 10^3 m^3/s	Temperature °C	Density* x 10^2 kg/m^3	Standard Deviation x 10^2	Total Spread x 10^2
118	.75	1.034	.269	22	6.48 ± 3.2%		
119	.75	1.034	.269	22	6.56 ± 3.1%		
120	.75	1.034	.272	22	6.29 ± 3.3%		
121	.75	1.034	.272	21	6.79 ± 3.0%		
122	.75	1.034	.273	21	6.80 ± 3.0%		
123	.75	1.034	.271	21	6.92 ± 3.0%		
124	.75	1.034	.271	21	6.61 ± 3.1%		
Mean	.75	1.034	.271	21	6.64	.22	.63
125	.75	1.276	.303	21	7.20 ± 2.9%		
126	.75	1.276	.303	21	7.42 ± 2.8%		
127	.75	1.276	.302	21	7.45 ± 2.8%		
129	.75	1.276	.302	21	7.19 ± 2.9%		
Mean	.75	1.276	.303	21	7.32	.14	.26
130	1.00	1.034	.273	22	5.91 ± 3.2%		
131	1.00	1.034	.273	22	5.91 ± 3.2%		
Mean	1.00	1.034	.273	22	5.91	0	0
132	1.00	1.276	.304	22	6.06 ± 3.2%		
133	1.00	1.276	.303	21	5.80 ± 3.3%		
134	1.00	1.276	.303	22	5.91 ± 3.2%		
Mean	1.00	1.276	.303	22	5.92	.13	.26
135	1.26	1.034	.271	21	5.72 ± 3.4%		
136	1.26	1.034	.271	22	6.38 ± 3.1%		
137	1.26	1.034	.270	22	6.24 ± 3.1%		
138	1.26	1.034	.270	22	5.86 ± 3.3%		
Mean	1.26	1.034	.271	22	6.05	.31	.66
139	1.26	1.276	.301	22	5.56 ± 3.5%		
140	1.26	1.276	.302	22	5.70 ± 3.4%		
Mean	1.26	1.276	.302	22	5.63	.10	.14

*Percent error shown in this column is due to counting statistics only.

TABLE 7

Data for Single Nozzle #1713A Centered Above X-Ray Beam

Test #	Height Above Beam m	Flow Rate x 10^3 m^3/s	Temperature °C	Density* x 10^2 kg/m^3	Standard Deviation x 10^2	Total Spread x 10^2
231	.72	.631	24	2.34 ± 4.3%		
232	.72	.631	24	2.63 ± 3.8%		
233	.72	.631	24	2.94 ± 3.4%		
234	.72	.631	24	2.72 ± 3.7%		
Mean	.72	.631	24	2.66	.25	.60
235	.72	.946	24	3.36 ± 3.0%		
236	.72	.946	24	3.16 ± 3.2%		
237	.72	.946	24	3.14 ± 3.2%		
Mean	.72	.946	24	3.22	.12	.22
229	.98	.631	25	2.32 ± 4.3%		
230	.98	.631	25	2.45 ± 4.0%		
Mean	.98	.631	25	2.39	.09	.13
226	.98	.946	25	3.30 ± 3.0%		
227	.98	.946	25	2.78 ± 3.6%		
228	.98	.946	25	3.05 ± 3.3%		
Mean	.98	.946	25	3.04	.26	.52
224	1.23	.631	26	2.06 ± 4.6%		
225	1.23	.631	26	2.19 ± 4.3%		
Mean	1.23	.631	26	2.13	.09	.13
222	1.23	.946	26	2.42 ± 4.0%		
223	1.23	.946	26	2.54 ± 3.8%		
Mean	1.23	.946	26	2.48	.08	.12

*Percent error shown in this column is due to counting statistics only.

Effect of Surfac... With...

Height Above Ream m	Without Surfactant: Mean Flow Rate x10^3 m^3/s	Without Surfactant: Mean Density x10^2 kg/m^3	Mean Flow Rate x10^3 m^3/s	Mean Density x10^2 kg/m^3
.75	.150	4.97	.148	4.59
.75	.165	5.20	.164	4.77
1.26	.148	4.42	.149	4.74
1.26	.165	5.03	.162	4.97

Data are for six Spraco nozzles #11062004.

TABLE 8

Effect of Surfactant on Measured Droplet Density

	Without Surfactant		With Surfactant	
Height Above Beam m	Mean Flow Rate $x10^3$ m^3/s	Mean Density $x10^2$ kg/m^3	Mean Flow Rate $x10^3$ m^3/s	Mean Density $x10^2$ kg/m^3
.75	.150	4.97	.148	4.59
.75	.165	5.20	.164	4.77
1.26	.148	4.42	.149	4.74
1.26	.165	5.03	.162	4.97

Data are for six Spraco nozzles #11062004.

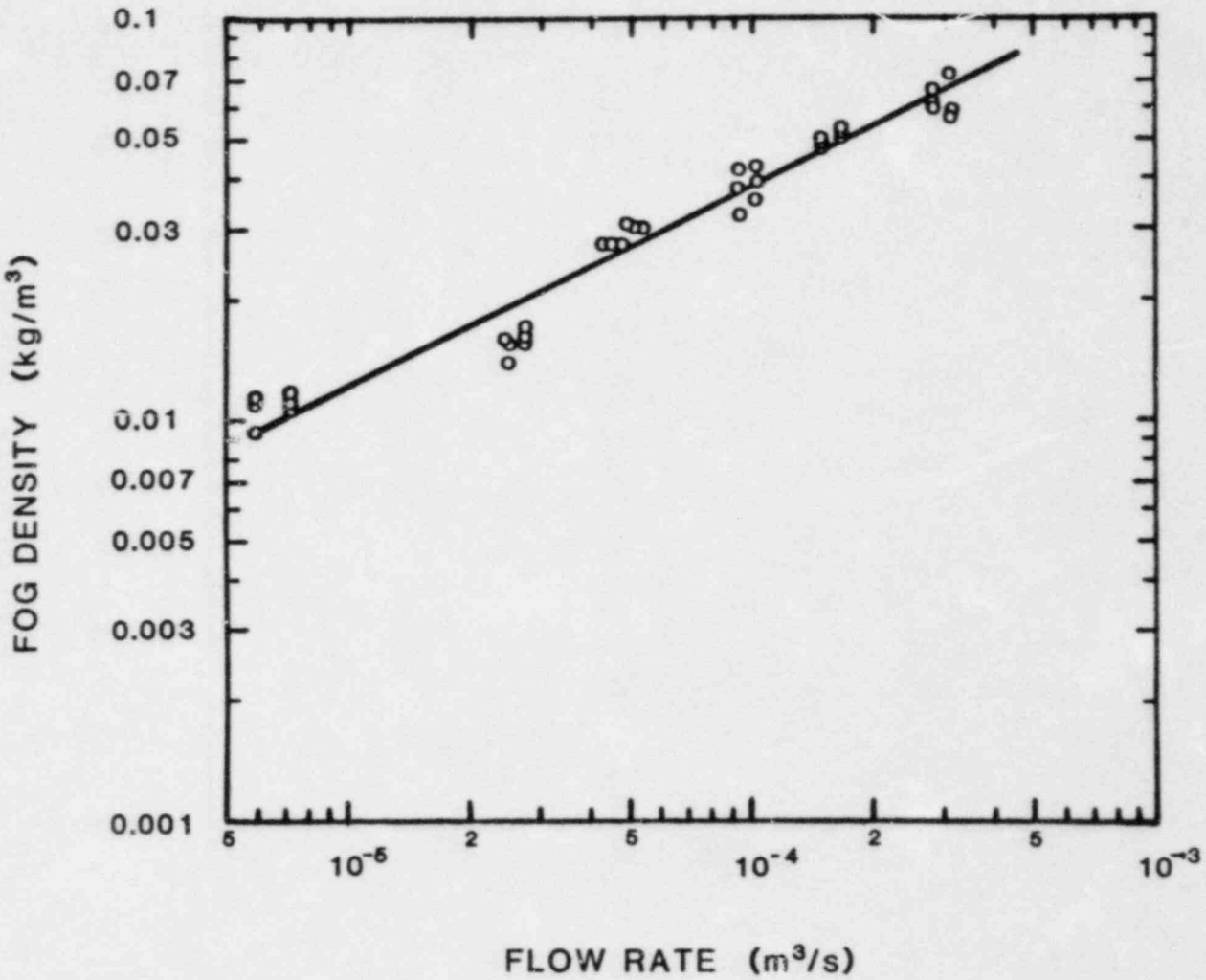

Figure 13. Density Versus Flow Rate for Nozzles #16030804 and #11062004

$$\rho = 6 \left(\frac{Q}{A}\right)^{1/2} \qquad (5)$$

where

ρ = fog density, kg/m^3

Q = flow rate, m^3/s

A = floor area, m^2

For the Sequoyah plant with a floor area of approximately 930 m^2, a flow rate of 0.26 m^3/s is required to achieve a density of 0.1 kg/m^3 (0.01 volume %). To achieve a density of 0.5 kg/m^3 (0.05 volume %), a flow rate of 6.5 m^3/s would be required.

Results for Nozzle #1713A

Table 7 shows the results for a single Spraco hollow-cone nozzle #1713A. This nozzle is currently in use in some nuclear plant containment buildings, including the Sequoyah plant. The #1713A nozzle produces drops with a mass mean radius of about 200 μm. Provided that there are some drops in the spray that are much larger than this (the drop size distribution is approximately log-normal), some self shielding of the drops is probably taking place. Therefore, the results in Table 7 may be low by a few percent (this is only an estimate).

One additional problem with the #1713A nozzle is that the drops have probably not slowed down to terminal velocity by the time they reach the x-ray beam. Calculations of velocity performed using equations 3 and 4 indicate that a drop of radius 200 μm will be falling at about 2.87 m/s when it reaches the beam, assuming a fall height of 1.23 m. The terminal velocity in stagnant air for such a drop is about 1.5 m/s. Since the density is inversely proportional to the velocity, the density could be significantly larger for a greater fall distance.

The decrease in density with increasing fall distance that is apparent in Table 7 is due primarily to geometric effects. As the nozzle is raised, more of the cone of spray is lost to the walls.

Due to the effects described above and the uncertainties associated with them, extrapolation of the #1713A data is somewhat precarious. However, using the data in Table 7 for 1.23 m and 9.46×10^{-4} m^3/s and assuming an increase of a factor of two to account for velocity effects, some rough estimates can be made using the following equation.

$$\rho = 2.5 \left(\frac{Q}{A}\right)^{1/2} \text{ kg/m}^3 \qquad (6)$$

For the Sequoyah plant, a flow rate of 1.5 m^3/s would be required to achieve a density of 0.1 kg/m^3 (0.01 volume percent). With the existing spray system at Sequoyah capable of producing only 0.852 m^3/s, equation (7) predicts a density of about 0.075 kg/m^3 (0.075 volume percent). While the numbers presented here are very tentative, it does appear that higher flow rates would be required for the #1713A nozzle than for the two nozzles described earlier.

Results with Surfactant

The final set of experiments, presented in Table 8, involved the addition of a surfactant to the water. In this case, 3 percent Akron Ultra High Expansion Synthetic Wet Water Foam Liquid - Style No. 999 was added to the water. This reduced the surface tension by a factor estimated to be 3 or 4. However, as shown in Table 8, the results do not indicate any major changes in density, indicating that there were no major changes in the agglomeration rates for this reduction in surface tension. These results are preliminary in nature, as other types of surfactants or methods for increasing the surface tension may produce different results.

As a final note, it should be clearly understood that the extrapolations performed using equations (5) and (6) in this section are useful for qualitative comparisons only. The reader should not attempt to use these equations to produce absolute quantitative numbers for a particular containment. The effects of large scale are certain to be significant, and extrapolation is risky at best.

VI. CONCLUSIONS AND RECOMMENDATIONS

Conclusions

Based upon the results presented in Section V, we have reached the following conclusions:

Flow Rate

The flow rate appears to be the dominant variable, with the density varying as the square root of the flow rate. This square root dependence instead of a linear dependence indicates that significant agglomeration is occurring.

Nozzle Type

Some differences were noted between nozzles producing drops with a mass mean radius of 200 μm and those producing drops with a mass-mean radius of 50 μm, with the smaller drops achieving densities a factor of two or three higher than the larger drops. However, further reducing the drop size to 25 μm seemed to have little effect. This suggests that there is a point of diminishing returns and that little gain in density will be achieved if the drop size is further reduced.

Nozzle Configuration

The nozzle configuration seemed to have little impact, except as it affected the flow rate. This may not be true for more closely packed nozzle arrangements, where nozzle interactions are more important.

Nozzle Height Above the Beam

In most cases, increasing the height slightly reduced the density. It is not clear whether these differences are due to increased agglomeration or increased wall losses. The answer may be a combination of both. The effects of height should be much more pronounced in large-scale experiments or reactor containments.

Surface Tension

The surfactant used in this experiment reduced the surface tension by a factor of 3 or 4, but had little effect on the fog density. This may not be true for all types of surfactants.

Recommendations

The experiments presented in this report represent a first step in ascertaining the feasibility of using water fogs as a hydrogen mitigation scheme. In order to provide conclusive recommendations regarding water fogs, we recommend performing the following tasks:

1. Develop methods for further characterizing the water fogs. Drop size information is critical in understanding the behavior of the fog. A promising laser technique under development is described in Reference 3. Another method under consideration involves direct droplet sampling by examining the impingement of drops on a layer of magnesium oxide (see Reference 4). It should also be noted that the x-ray equipment used in this experiment is not portable, further reinforcing the need to develop other techniques.

2. Conduct experiments at a larger scale. These experiments will be necessary to adequately understand the effects of geometry and fall height and to be able to make accurate predictions for reactor containments.

3. Conduct combustion tests in the presence of fogs. A better understanding of the effects of fogs upon combustion (quenching, flame acceleration, etc.) is needed.

REFERENCES

1. M. Berman, M. P. Sherman, J. C. Cummings, M. R. Baer, and S. K. Griffiths, "Analysis of Hydrogen Mitigation for Degraded Core Accidents in the Sequoyah Nuclear Power Plant," NUREG/CR-1762, SAND80-2714, Sandia National Laboratories, Albuquerque, NM (March 1981).

2. L. W. Morrison and K. M. Glibert, "Sandia National Laboratories' Henke X-Ray System," Sandia National Laboratories, Albuquerque, NM (July 1974).

3. M. Berman, "Light Water Reactor Safety Research Program Semiannual Report, April-September 1981," NUREG/CR-2481, SAND82-0006, Sandia National Laboratories, Albuquerque, NM (February 1982).

4. K. R. May, J. Sci. Instr. 27, 128-130 (1950).

DISTRIBUTION:

U. S. NRC Distribution Contractor (CDSI) (345)
7300 Pearl Street
Bethesda, MD 20014
320 copies for R3
25 copies for NTIS

Author selected distribution -
(List available from author)

1513 - M. R. Baer
1513 - S. K. Griffiths
1513 - S. N. Kempka
1513 - A. C. Ratzel
2513 - J. E. Shepherd
2513 - S. F. Roller
9441 - M. Berman (15)
9441 - A. L. Camp (15)
9441 - J. C. Cummings
9441 - S. E. Dingman
9441 - D. E. Mitchell
9441 - L. S. Nelson
9441 - P. G. Prassinos
9441 - D. J. Rzespecki
9441 - M. P. Sherman
9441 - S. R. Tieszen
9441 - M. J. Wester
3141 - L. J. Erickson (5)
3151 - W. L. Garner (3)

120555078877 1 ANR3
US NRC
ADM DIV OF TIDC
POLICY & PUBLICATIONS MGT BR
PDR NUREG COPY
LA 212
WASHINGTON DC 20555

Org.	Bldg.	Name	Rec'd by	Org.	Bldg.	Name	Rec'd by

Sandia National Laboratories